The myth of softening behavior of the cohesive zone model exact derivation of yield drop behavior of wood

van der Put, Tom

Publication date
2015

Document Version
Final published version

Published in
International Journal of Computational Engineering Research (IJCER)

Citation (APA)
van der Put, T. (2015). The myth of softening behavior of the cohesive zone model exact derivation of yield drop behavior of wood. *International Journal of Computational Engineering Research (IJCER)*, *5*(11), 29-43.

ISSN (e): 2250 – 3005 || Volume, 05 || Issue, 11 ||November – 2015 ||
International Journal of Computational Engineering Research (IJCER)

The Myth of Softening behavior of the Cohesive Zone Model Exact derivation of yield drop behavior of wood

T.A.C.M. van der Put
TU Delft, Civil Engineering and Geosciences; Timber structures and wood technology -

Abstract:
It is shown that the postulate of strain softening of the fracture stress is based on the error to regard the nominal stress to be the actual, ultimate stress, at the actual area of the fracture plan. Strain softening called yield drop is elastic unloading of the actual elastic stress at the intact, not ltimate, elastic loaded part of the specimen, outside the fracture zone. It appears that the Griffith theory only applies for the first yield drop until half unloading and further fracture follows from a ultimate stress criterion A small-crack merging mechanism explains precisely the "softening" called yield drop curve.

Keywords: *wood, timber, fracture mechanics, limit analysis, strain softening, yield drop, fictitious crack model, cohesive zone model, continuum damage mechanics, small crack merging mechanism, molecular deformation kinetics,*

I. Introduction

The application of the (structural impossible) strain softening postulate for fracture, is strictly against theory, and results, since long, in a tremendous spill of research efforts, without any possibility of progress. The lack of theory is also leading to models (see e.g. the German controlled CIB-W18 papers), where all viscoelastic, plastic, and structural change processes in e.g. beam type specimens at loading, (which are known from molecular deformation kinetics [1]), are regarded as one fracture process. This results in a never ending stream of publications of assumed R-curves. The non-existence of the hardening R-curve for wood is nevertheless known from relevant small- and plate specimen data, showing no kinks in the loading line, while the kinks at mode II loading of edge notched beams is shown in [2] to be due to necessary plastic stress redistribution.

Despite this assumed hardening, a softening transformation is assumed at crack extension. This softening postulate leads to impossible models, e.g. with negative spring constants, anti-normality, negative dissipation, etc., all strictly against admissibility and against the possibility to predict strength in any circumstance. The last representative of this ineffectual movement is the cohesive zone model, which is, as all the applied empirical models, based on the general error to regard the nominal stress to be the actual stress at the fracture plane.

To try to correct this convincingly in the light of exact theory, it will be shown that real strain softening does not exist, and thus is not a material property. Yield drop (wrongly called softening) is only possible in a constant strain rate test, when the rate of the unloading process is higher than the loading rate by the constant strain rate test. Yield drop ("softening") therefore is not possible in a constant loading rate test and also not in a dead load to failure test. Also when instability is involved in the dead load test, yield drop is not possible. "Strain softening" thus, is not "softening", but is elastic unloading of the actual stress of the intact, not ultimate loaded, part of the specimen, thus outside the fracture region. Apparent and real (e.g. thermal) softening are fully described by (exact) deformation kinetics [1], without the need of impossible physical properties. It will be shown, that the real, actual stress at the fractured plane never is able to show yield drop and always determines strength behavior, what involves that deformation kinetics always has to be applied.

II. Discussion of the Fictitious crack models

The cohesive zone model is mostly qualified as a (Hillerborg type) fictitious crack model, thus is based on a fictive crack length extension, which is loaded by a cohesive flow stress, over such a length that the singularity due to this cohesive flow stress neutralizes the singularity due to the field stress at the extended crack tip. The extended crack length is however not fictitious, but real, because only then, there is a real singularity possible at a real extended crack tip, which can be neutralized. The singularity is not neutralized at the existing crack tip when this crack extension is not real. Calculated thus is the strength of an extended crack length in a stress field, loaded also by a physical and structural not possible internal opposite applied, liquid-like, viscous soften-

ing stress field near the crack tips. Although the aim of the fictitious crack models (Dugdale, Barenblatt, Hillerborg) initially was, to remove the infinite high stresses of the singularity approach, it later simply was assumed, that by the fictive softening boundary condition, the strength, of the real crack tip singularity, approaches zero, in stead of going to infinity.

These approximation models, with arbitrary outcomes (due to the impossible, now arbitrary chosen, softening boundary condition and wrong failure criterion), need not to be followed, because it is not necessary to choose an approximation of an approximation. Thus to choose a correction on the singularity solution of the Airy stress function. In chapter 2 of [2] the exact boundary value limit analysis approach, without singularities, is presented, leading to an exact Wu-failure criterion. The same can not be derived by the, singularity methods, which lead to an ultimate stress criterion for combined loading. Thus mode I and/or mode II failure is predicted to be determining, depending on which critical value of the two is the first reached. Thus an up to 100 % overestimate of the strength is in principle possible as follows from the exact (Wu-) equation, and the singularity method and the thereupon based fictitious crack models, thus are not exact for the mixed mode loading case.

The most near to exact, for uniaxial loading, is, (according to elastic-plastic limit analysis), the Dugdale method, and the results can be compared with the results of the exact solution. Then, the extended crack length r_p, according to the Dugdale model is:

$$r_p = \frac{\pi}{8} \cdot \left(\frac{K_{Ic}}{\sigma_f} \right)^2 = \frac{\pi^2 \sigma^2 c}{8 \sigma_f^2}, \tag{2.1}$$

where σ_f is a yield stress. This leads to a maximal crack opening displacement δ_c at the crack tip of:

$$\delta_c = \frac{8}{\pi E} \cdot \sigma_f \cdot r_p = \frac{K_{Ic}^2}{E \sigma_f} = \frac{\pi \sigma^2 c}{E \sigma_f} \tag{2.2}$$

when r_p from eq.(2.1) is substituted. This result, based on singularity equations, was necessarily based on very small values of r so that all terms (of the Airy stress function solution) containing not the factor $r^{-0.5}$ were neglected at the derivation of the solution equation. For finite values of r, and for the singularity neutralization effect by superposition of yield stresses, this is not allowed, leading to a not correct result. According to the exact theory, Chapter 2 of [2], applies, for Mode I, at the crack tip boundary r_0, at the start of flow, the condition: $r_0 = 2c\left(\sigma / \sigma_f\right)^2$, according to eq.(2.29) of [2] for the elliptic crack tip and applies approximately: $r_0 = c\sigma^2 / 2\sigma_f^2$ according to eq.(2.20) of [2] for the circular crack tip of the singularity approach, showing a difference by a factor 4, depending on neglected terms and form of the crack tip determining value of the tangential tensile stress along the crack-tip boundary. The Dugdale numerical factor: $\pi^2 / 8 = 1.23$ (based on an enlarged crack length) is between these values of 0.5 and 2, but is too far away from the elliptic value 2, which applies as highest lower bound of limit analysis (which bound is equal to the measurements, thus is the solution). Also the theoretical elastic elliptic crack opening displacement of: $\delta_c = (2\sigma c) / E$ is far above the Dugdale value. The Dugdale model thus shows a not exact, too low, thus rejectable, lower bound of the strength, which only applies for uniaxial loading.

A similar rejection applies for the Hillerborg cohesive zone model, which is based on "closing" stresses, proportional to the "softening" curve, because it wrongly is based on the nominal stress change, which is the decreasing elastic actual stress of the intact part, outside the fracture plane, and thus is not based, (as necessary for a right solution, see § 3, [1], [2], [3]), on the actual stress at the fracture plane, which is a, by stress spreading, [4], increasing, actual stress. Therefore, wrongly, a zero tangential stress is found at the location of the highest (strength determining) tangential tensile stress at the crack boundary. This error is of course opposite from right, as further discussed later, based on the exact derivation of the, "softening" called, yield drop curve.

III. Continuum damage mechanics

Continuum damage mechanics [3], is a simplified application of needed Deformation Kinetics analysis (of [1]), leading to the most elementary damage kinetics equations. Regarding fracture mechanics of [3], the analysis is based on the fractured (lost) area A of an initially undamaged section A_0, leading to the variable:

$$\psi = \frac{A_0 - A}{A_0} \tag{3.1}$$

The actual stress σ_a on the material then is (expressed, as wanted, in the nominal stress σ):

$$\sigma_a = \frac{P}{A_0 - A} = \frac{P}{A_0 \psi} = \frac{\sigma}{\psi} \tag{3.2}$$

where σ is the nominal stress and σ_a the actual tress on still undamaged (=actual) area of the section. Now:

- 1. The actual stress on the actual area evidently determines the rate of damage growth, and:
- 2. The strain increase due to damage is caused by the actual stress at the damage location.

Thus, the stress-strain behavior of the damaged material can be represented by the constitutive equation of the virgin, undamaged, material with the stress, in it, replaced by the actual stress. Thus:

$$\varepsilon = \frac{\sigma_a}{E} = \frac{1}{E} \cdot \frac{\sigma}{\psi} = \frac{\sigma}{E'} \tag{3.3}$$

with: $E' = E\psi$. A simple form of the deformation kinetics damage equation for uniaxial tension is:

$$\frac{d\psi}{dt} = -C\left(\frac{\sigma}{\psi}\right)^n \tag{3.4}$$

This is comparable with the deformation kinetics equation of [1] and § 5:

$$\frac{dN}{dt} = -CN_0 \exp\left(\frac{\sigma\lambda'}{kN}\right), \tag{3.5}$$

for a forward zero order reaction due to high stress, where the exponential equation is replaced by its power law representation in eq.(3.4). (See for that last: Section 4.4 of [2]).

To apply this, for a rod, loaded by a constant tensile stress σ_0 , the initial boundary condition of eq.(3.4), for a virgin material, is: $\psi = 1$ at $t = 0$, while at complete fracture: $\psi = 0$.

Integration of eq.(3.4) then gives for the time to failure: $t' = \left[C(n+1)\sigma_0^n\right]^{-1}$.

For stepwise loading then follows:

$$\sum_{k=1}^{s} \frac{\Delta t_k}{t'_k} = 1; \quad t'_k = \left[C(n+1)\sigma_k^n\right]^{-1} \text{ with: } \Delta t_k = t_k - t_{k-1}, \qquad \text{k} = 1,2,\ldots..\text{s.} \tag{3.6}$$

which is Miner's rule, or the principle of linear summation, which evidently also applies for wood and timber. Important conclusions now are:

1. It is necessary to apply of the actual stress in damage equations, for right results, as is applied in [3], [2] and [1], for all existing solutions, which all are empirically verified by tests, and:
2. Limit analysis deformation kinetics [1] has to be applied, (e.g. in continuum mechanics), for exact solutions. This is discussed and applied in next sections.

IV. Softening-like behavior and fracture energy

4.1 Introduction

The derivation of "softening"- called yield drop behavior of the Griffith stress, is discussed in [2], chapter 3 and it is shown that the area under this load-displacement yield drop curve, divided by the crack area, is not the fracture energy, but the total external work on the specimen. The fracture energy is half this value and is equal to the decreasing critical strain energy release rate along the yield drop curve. For wood this factor ½ is correctly is applied for mode II. For mode I this is not the case and a two times too high value is applied. According to the, for wood applied, Hillerborg, fictitious crack model, is the fracture energy related to the newly formed fractured area, what is not a right definition because the energy then is by definition different for different initial crack lengths and thus is undetermined. Necessary is to use the Griffith definition, which includes the energy of formation of the initial crack for the total energy of full crack extension over the whole width of the specimen.

Inconsistent, with the choice to relate the fracture energy to the actual newly formed fractured area, the fictitious crack model regards the nominal stress, (which is the actual elastic stress of the intact part of the specimen) to be the actual strength stress at de fracture plane. As consequence, the (by stress spreading increasing) strength, decreases strongly by definition, proportional to the yield drop curve at crack extension and approaches zero strength at the end what is against physics and against equilibrium conditions. Further, the success of the, deformation independent, Griffith theory, (and equilibrium method of limit analysis of [2]), with its constant apparent surface energy and constant energy release rate, is ignored, but should be explained by any new theory. It therefore also is necessary to discuss the real strain energy release rate at the top of the yield drop curve, which causes the start of macro-crack extension, but is shown to be determined by a critical small-crack density [2]. It further appears that proceeded small-crack extension also determines the "softening" curve and post fracture behavior, as discussed in the following.

4.2. Mode I, hardening and "softening"-like behavior

"Softening"- like yield drop only exists for the nominal stress and not for the actual fracture stress. The Griffith stress, eq.(4.8), is a nominal stress, acting on the section $b \cdot t$ of Fig. 4.1. This stress, therefore is in reality the actual stress of the intact, not fractured, part of this specimen, which shows "softening"- like yield drop, following the Griffith locus, what thus is not strain softening (at failure) but is unloading of intact undamaged material. The actual stress at the fractured section shows hardening and quasi hardening by stress spreading and thus no softening as will be derived below. The same applies for the necked actual cross section area of steel and for reduced area of other materials. Clearly the term strain softening has to be replaced by (dynamic) elastic unloading (when the unloading process is faster than the loading rate by the constant strain rate test).

As most materials, wood shows near failure a plastic and apparent plastic (deformation independent) behavior. Plasticity causes the apparent surface energy to be much higher than the real surface energy and when the test rig is stiff enough, the top of the loading curve is shown to be blunted enough to make any stress redistribution possible and the behavior can be approximated by equivalent elastic- full plastic behavior. Therefore limit analysis applies and linear elastic fracture mechanics can be applied, up to the ultimate stress at the elastic-plastic boundary around the crack tip. The dissipation by micro cracking, plastic deformation, and friction, within this boundary, called fracture process zone, then is regarded as part the fracture energy for macro crack extension. When a specimen is loaded until "flow", before the start of yield drop, and is then unloaded and reloaded, the behavior has really become elastic-full plastic, and the real stress differs an internal equilibrium system from the linear elastic loading stresses. According to the limit theorems, initial stresses or deformations have no effect on the plastic limit collapse load, provided the geometry is essentially unaltered and thus the calculation is based on initial dimensions. Therefore also, as method of practice and of the Building Codes, calculations can be based on a reduced E- modulus up to the ultimate state and therefore also the linear elastic derivation of the elastic unloading curve of the fractured specimen, is possible, based on the compliance method, as is followed below. It also should be realized that, for wood, confined plasticity, as e.g. occurs at ultimate bending compression, can be replaced by the equivalent linear elastic bending strength. Thus a linear elastic calculation up to the crack boundary is possible and the term: "linear elastic fracture mechanics" then is in fact a pleonasm.

In Fig. 4.1, a mode I, center notched test specimen is given with a length "l", a width "b" and thickness "t", loaded by a stress σ showing a displacement increase δ of the loaded boundary due to a small crack extension. The work done by the constant external stress σ on this specimen, during this crack extension is equal to:

$$\sigma \cdot b \cdot t \cdot \delta = 2W = 2\left(\sigma \cdot b \cdot t \cdot \delta / 2\right) \tag{4.1}$$

This is twice the increase of the strain energy W of the specimen. Thus the other half of the external work, equal to the amount W, is the fracture energy, used for crack extension. Thus the fracture energy is equal to half the applied external energy, which is equal to the strain energy increase W. This follows, for the total crack length, from the difference of the strain energy of a body containing the crack and of the same body, without a crack:

$$\frac{\sigma^2}{2E_{eff}} blt - \frac{\sigma^2}{2E} blt = W \tag{4.2}$$

The fracture energy is also equal to the strain energy decrease at fixed grips conditions when $\delta = 0$:

$$W = t\sigma \int_{-c}^{+c} v\,da = \pi\sigma^2 c^2 t / E \tag{4.3}$$

where the last two terms give the strain energy to open (or to close) the sufficient small, flat, elliptical crack of length $2c$ and where "v" is the virtual displacement of the crack surface in the direction of σ.
From eq.(4.2) and eq.(4.3) follows that:

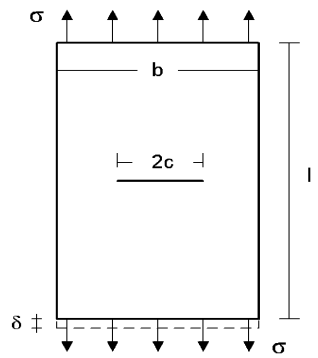

Figure 4.1 - Specimen b x l and thickness t, containing a flat crack of $2c$

$$\frac{\sigma^2}{2E_{eff}} blt - \frac{\sigma^2}{2E} blt = \pi\sigma^2 c^2 t / E \tag{4.4}$$

Thus the effective Young's modulus of the specimen of Fig.4.1, containing a crack of 2*c*, is:

$$E_{eff} = \frac{E}{1 + 2\pi c^2 / bl} \tag{4.5}$$

The equilibrium condition of the critical crack length is:

$$\frac{\partial}{\partial c}(W - G_c 2ct) = 0 \tag{4.6}$$

where G_c is the fracture energy for the formation of the crack surface per unit crack area.

With *W* of eq.(4.2) or of eq.(4.3), eq.(4.6) becomes:

$$\frac{\partial}{\partial c}\left[\frac{\pi\sigma^2 c^2 t}{E} - G_c 2ct\right] = 0, \quad \text{or:} \quad \frac{\partial}{\partial c}\left[\frac{\sigma^2 blt}{2E}\left(1 + \frac{2\pi c^2}{bl}\right) - \frac{\sigma^2 blt}{2E} - G_c 2ct\right] = 0 \tag{4.7}$$

giving both the nominal Griffith strength:

$$\sigma_g = \sqrt{\frac{G_c E}{\pi c}} \tag{4.8}$$

This stress is the actual stress P / bt outside the fractured section and is a nominal stress for the fractured section, related to the width *b* of the specimen of Fig. 4.1. The real, actual, mean stress in this weakest actual cross section (ligament) with width: $b - 2c$, where fracture occurs, is:

$$\sigma_a = \sqrt{\frac{G_c E}{\pi c}} \cdot \frac{b}{b - 2c} = \sqrt{\frac{G_c E}{\pi b}} \cdot \frac{1}{(\sqrt{c / b}) \cdot (1 - 2c / b)} \tag{4.9}$$

Because this stress is determining for newly formed crack area, it is applied by the fictitious crack models for a local fracture energy estimation. It is however not noticed that this use of the actual stress leads to "hardening", in stead of "softening", according to:

$$\frac{\partial \sigma_a}{\partial(\sqrt{c / b})} = \sqrt{\frac{G_c E}{\pi b}} \cdot \frac{6c / b - 1}{(c / b) \cdot (1 - 2c / b)^2} > 0 \tag{4.10}$$

This occurs when *c/b* > 1/6, what always is the case for actual critical crack lengths. The real actual stress σ_a increases with the increase of the crack length even up to infinity when 2*c* approaches *b* and hardening behavior characterizes the critical stress. However, there is a maximal value for this clear wood fracture as discussed in § 6. This constant maximal value of the energy release rate for each mode is basic for the Griffith theory. Then the nominal stress follows the Griffith locus, eq.(4.12) (see Fig. 4.6), as failure condition, which also is the condition of no damage acceleration, and the applied strain rate, at the end of the test is relatively slow, so that it has to be increased highly, (by one order in [5]), to shorten the delay time of the macro crack fracture process.

The stress for e.g. the minimal critical crack length of *c/b* = 1/6, is: $\sigma_c = \sqrt{G_c E / \pi c} = \sqrt{G_c E / (\pi\, b / 6}$ and the actual stress at the fracture plane is: $\sigma_{c,u} = \sqrt{G_c E / (\pi\, b / 6)}\, b(/(b - b)) = 1.5\sqrt{G_c E / (\pi b / 6)}$.

Thus is 1.5 times the nominal Griffith stress. Thus, macro crack extension demands an increase of the tensile strength. The possible tensile strength increase, follows from the exact stress spreading theory of [4]. Although derived for local compression, the sign of the shear stresses may be reversed and the same spreading rules apply for tension. For *c/b* = 1/6, according to Fig. 4.1, there is a spreading of the stress on 4*c* solid material to: $b = 6c$. Thus the tensile strength is: $\sqrt{6 / 4} \cdot \sigma_m = 1.22 \cdot \sigma_m$, thus 1.22 times the uniaxial tensile strength σ_m. The nominal, fully spread, stress then is $\sqrt{4 / 6} \cdot \sigma_m = 0.82 \cdot \sigma_m$. Thus a factor 1.5 lower. High peak factors occur at long initial cracks, but there is a maximal value due to maximal possible spreading. Also the fully spread stress remains too high to explain macro crack extension at low mean stresses, where also the fracture energy is too low. Thus total fracture can not be due to single macro crack extension alone (see § 4.7). As known, a system of small cracks in the ligament, may lower the load of the adjacent intact, undamaged, part of the specimen and a high concentration of small cracks appears to be necessary to explain fracture at low nominal stresses. Because unloading is determined by the decrease of stiffness of the specimen, by crack extension, the mathematical expression of this influence has to be derived. This is discussed in the next paragraph 4.3.

4.3. The "softening"- called, yield drop curve

"Softening" (yield drop) should be described by Deformation Kinetics [1] but an alternative description of the so called "softening" behavior as a result of former crack propagation alone is possible by the Griffith theory, which can be regarded as an equilibrium method of limit design. Straining the specimen of Fig. 4.1 to the ultimate load at which the initial crack will grow, gives, according to eq.(4.5):

$$\varepsilon_g = \sigma_g / E_{eff} = \sigma_g \cdot \left(1 + 2\pi c^2 / bl\right) / E \tag{4.11}$$

Substitution of $c = G_c E / \pi \sigma_g^2$, of the ultimate state, according to eq.(4.8), gives:

$$\varepsilon_g = \sigma_g / E + 2G_c^2 E / \pi \sigma_g^3 bl \tag{4.12}$$

This is the equation of critical (unstable) equilibrium states, representing the apparent softening (= unloading) curve, due to the Griffith stress, eq.(4.8), which is the actual stress on the intact part of the specimen, outside the fracture plane. It is shown by the dynamics of crack propagation that the velocity of crack propagation is zero at the initial critical crack length and that the Griffith relation, eq.(4.8), is the condition for zero acceleration of crack extension. Thus the crack of Griffith length is in unstable equilibrium but does not propagate. The "softening"- called yield drop curve, eq.(4.12), is known as "Griffith locus" and has a vertical tangent $d\varepsilon_g / d\sigma_g = 0$, occurring at a crack length of:

$$c_c = \sqrt{bl / 6\pi}\ , \tag{4.13}$$

which is the top of the curve. Smaller cracks than c_c are unstable because of the positive slope of the locus (see eq.(4.16), because crack recovery is not possible). These small cracks, (if any, near the macro-crack tip) extend during the loading stage, by the high peak stresses at the notch of the test specimen, to a stable length and only higher crack lengths than c_c are to be expected at the highest stress before yield drop, giving the stress-strain curve of Fig. 4.2 with σ_c of eq.(4.15) as top value. For a distribution of small cracks, in a repeating pattern, *b* and *l* in eq.(4.13) are the St. Venant crack distances and the critical crack distance for extension is about 2.2 times the crack length. Because, when $b \approx 2.2 \cdot (2c_c)$ and: $l \approx 2.2 \cdot (2c_c)$, then: $bl \approx 19 \cdot c_c^2 \approx 6\pi\ c_c^2$ according to eq.(4.13). This also applies for extended small cracks after merging because the stress flow around the crack needs the St Venant's distance below the crack to be on full strength and to be able to extend the there present small cracks further. Thus the critical crack density, for the start of yield drop, is reached, when the small crack distance is about the crack length. This critical distance also is predicted by Deformation Kinetics, discussed in § 5, and is used in § 4.6 to explain yield drop by small-crack propagation in the fracture plane (at the ligament).

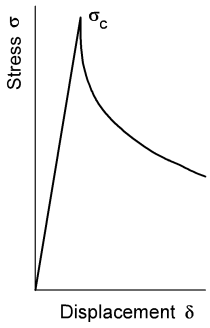

Figure 4.2 – "Softening" curve according to eq.(4.12) for the specimen of Fig. 4.1 or 4.5.

According to eq.(4.13), the yield drop line, eq.(4.12), now can be given as:

$$\varepsilon_g = \frac{\sigma_g}{E}\left(1 + \frac{\sigma_c^4}{3\sigma_g^4}\right), \tag{4.14}$$

where: $\sigma_c = \sqrt{E G_c / \pi c_c}$ (4.15)

is the ultimate load with c_c according to eq.(4.13). The negative slope of the Griffith locus is:

$$\frac{\partial \sigma_g}{\partial \varepsilon_g} = -\frac{E}{\frac{\sigma_c^4}{\sigma_g^4} - 1} \tag{4.16}$$

Vertical yield drop occurs at $\sigma_g = \sigma_c$, and the strain then is: $\varepsilon_{gc} = (\sigma_c / E) \cdot (1 + 1/3)$ and eq.(4.14) becomes:

$$\frac{\varepsilon_g}{\varepsilon_{gc}} = 0.75 \cdot \left(\frac{\sigma_g}{\sigma_c} + \frac{\sigma_c^3}{3\sigma_g^3} \right), \tag{4.17}$$

More in general eq.(4.14) can be written, when related to a chosen stress level σ_{g1}:

$$\frac{\varepsilon_g}{\varepsilon_{g1}} = \frac{\sigma_g}{\sigma_{g1}} \cdot \frac{1 + \sigma_c^4 / 3\sigma_g^4}{1 + \sigma_c^4 / 3\sigma_{g1}^4} \tag{4.18}$$

To control whether σ_c changes, eq.(4.18) can be written like:

$$\frac{\sigma_c}{\sigma_{g1}} = \left(\frac{3 \cdot (\sigma_g / \sigma_{g1})^3 \cdot \left((\varepsilon_g / \varepsilon_{g1}) - (\sigma_g / \sigma_{g1}) \right)}{1 - (\varepsilon_g / \varepsilon_{g1}) \cdot (\sigma_g / \sigma_{g1})^3} \right)^{0.25} \tag{4.19}$$

with the measured values at the right hand side of the equation. When the occurring "softening" curve starts to differ from the Griffith locus, σ_c decreases, causing a steeper decline of the curve, due to additional small crack and clear wood failure of the fracture plane. This failure by a small-crack merging mechanism is discussed in § 4.6. To measure the fracture energy as area under the softening curve, the displacement of the loading jack due

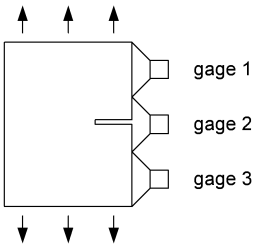

Figure 4.3. Measuring nonsense data at gage 2

to the mean deformation of the specimen has to be known. This can not be obtained by measuring the gage displacement over an crack opening (see Fig. 4.3) because it is not known what then is measured and this local unloading, around the open crack, is mainly proportional to the crack length itself, and is not simply related to the constant ultimate stress state of the ligament.

4.5. Empirical confirmation

The measurements of [5] are complete by measuring the whole loading and yield drop curve and using the compact tension tests as control, being also a control by the different loading case. The graphs of [5], Fig. 4.6 and 4.7, are the result of tension tests on the specimen of Fig. 4.5. The length of the specimen was l = 3 mm, the width and thickness: $b = t$ = 20 mm and the notch length $2c$ = 2x5 = 10 mm with a notch width of 0.5 mm. In figures 4.6 and 4.7, measured stress-displacements are given together with the lines 1 and 2 according to Griffith locus: eq.(4.17). The strain ε_g follows from the displacements at the x-axis of the figures, divided

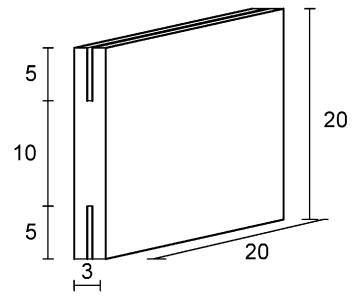

Figure 4.5 - Geometry of the specimens [5]

through 3 mm, the measuring length and length of the specimen. Because of the small length of 3 mm, not the whole width b of the specimen is active. Assuming a possible spreading of 1.2:1, through the thickness of 1.25 mm above and below the side notches, the working width b_{eff} is equal to the length of the fracture plane plus 2 times 1.2 x 1.25 or b_{eff} = 10 + 3 = 13 mm.

Thus the notch lengths in Fig. 4.5 should be regarded to be 1.5 mm in stead of 5 mm. The stresses in the figures 4.6 and 4.7, are related to the length of the fracture plane, thus are actual stresses and are not related to b_{eff} according to the nominal Griffith stress, wherefore the actual stresses have to be reduced by a factor: 10/13 = 0.77, as done and discussed in [2].
Macro crack extension occurs by small crack merging with the macro crack tip. Thus is due to small-crack propagation toward the macro-crack tip. The level above 4 (to 4.6) MPa is measured in 3 of the 10 specimens of the discussed series T1309/2309 of [5] and an example is given in Fig. 4.6, reaching the top of Fig. 4.2, indicating that this strength of the fracture plane according to crack-pattern A of fig. 4.8 was determining for yield drop. The other specimens of this series did show lower strength values than about 4 MPa, as applies for further unloading due to already extended small cracks.

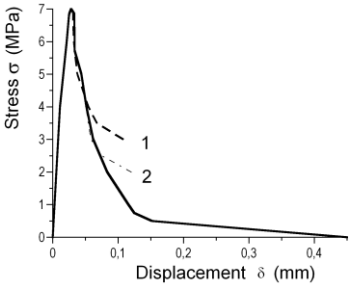

Figure 4.6 - Stress - displacement of specimen T 1409 of [5].

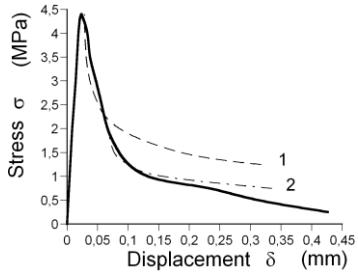

Figure 4.7 - Stress - displacement of specimen T 1509 of [5]

At § 4.3 and § 5 is shown that for the critical small crack density of eq.(4.13), the crack distance is about the crack length, as given by row A of Fig. 4.8. Line 1 of Fig. 4.6 gives the primary crack extension, eq.(4.17), by this critical crack density. Curve 1 levels off from the measurements at σ = 4 Mpa, where the next process starts, given by line 2. This thus happens when the crack length has become about 3 times the initial critical value $c_{c,0}$, according to

$$\sigma_g = \sqrt{\frac{E G_c}{\pi 3 c_{c,0}}} = 0.57 \cdot 7 = \cdot 4 \text{ MPa} \qquad (4.20)$$

This 3 times larger crack length is given by crack row B of Fig. 4.8. The top value σ_c of the first process on row A, is σ_c = 7 Mpa, for all values of σ_g between 4 and 7 Mpa. The top value of the second process B on $3c_{c,0}$ cracks, is: σ_c = 4 MPa. This process ends, where cracks of $7c_{c,0}$ lengths remain, according to row C of Fig. 4.8. Thus when:

$\sigma_g = \sqrt{\frac{E G_c}{\pi 7 c_c}} = \frac{1}{\sqrt{7}} \sqrt{\frac{E G_c}{\pi c_c}} = \frac{1}{\sqrt{7}} \cdot 7 = 0.378 \cdot 7 = 2.65$ Mpa (where line 2 of Fig. 4.6 levels off from the data)

This stress is equal to top value σ_c of the next process C, on $7c_{c,0}$ cracks, given below line 2 in Fig. 4.6. This ends at: $(1/\sqrt{15}) \cdot 7 = 0.258 \cdot 7 = 1.81$ Mpa, where the process on 15 $c_{c,0}$ starts. However, processes towards the longer cracks of 15, 31 and 63 $c_{c,0}$ are not distinct and it is probable that, due to the high actual stress, failure may occur at any point of the still intact part of the ligament.

Again, due to the spreading effect very high tensile stresses are theoretically possible, but overcritical crack lengths just show empirically too low K_{Ic} values, showing the Griffith strength and critical energy release rate to be not followed. Thus failure by post-critical crack lengths is due to ultimate uniaxial clear wood tensile stress, (or shear stress for mode II) and is not due to a critical release rate. This will be discussed further at § 4.7.

It now is shown, that the Griffith yield drop equation, combined with the crack merging model, precisely explains the data of strong specimens. The data of the less strong specimens, given by Fig. 4.7, show instability of process A, due to the steep slope near the top of Fig. 4.2. (This also explains the high variability found in [5]). Line 1 of Fig. 4.7 is the same as line 2 of Fig. 4.6, and can be chosen to level off at about 2.2 MPa, in accordance with the uniaxial strength of the still intact area of the ligament, which is half the area at 4.4 MPa, showing again that an ultimate stress criterion is determining above the nominal Griffith strength criterion for long small-cracks (thus at low nominal stress). The crack merging mechanism, clearly noticeable at strong specimens, is a chosen lower bound equilibrium system of limit analysis, which precisely follows the measured data (See § 4.6).

4.6. Crack merging mechanism

The increased unloading (yield drop), with respect to macro crack extension due to small crack extension, at the fracture plane, can be explained, using the equilibrium method, by the joining of the small cracks as follows:. In § 4.3 and § 5 it is shown, that the critical intermediate small crack distance, for crack extension, is about equal to the crack length, as given in scheme A below. In § 4.3, a crack distance of 2.2 times the crack length is found, what for simplicity of the model is rounded down here to 2, giving slightly too high stresses. For these small cracks, the critical crack length according to eq.(4.13) then is:

2c 2c 2c 2c 2c 2c 2c 2c 2c 2c 2c 2c 2c 2c . A

6c 2c 6c 2c 6c 2c 6c . B

14c 2c 14c . C

Figure 4.8. Small crack merging

$c_c = \sqrt{lb/6\pi} = \sqrt{2.2\cdot(2c_0)\cdot 2.2\cdot(2c_0)/(6\pi)} = 1.0\cdot c_0$, for the specimen with row A.

The distance *l* between the rows, above each other, is 2.2 times the crack length, being the Saint-Venant distance for building up the stress again behind a crack, to be able to form a new crack. Thus $l = b = 2.2\cdot 2c$ for row A, and $l = b = 2.2\cdot 6c$ in row B, and $l = b = 2.2\cdot 14c$ for row C. Thus when crack pairs of row A join together, a crack length of 6*c* occurs. The critical crack length thus is for row B:

$c_c = \sqrt{lb/6\pi} = \sqrt{2.2\cdot 6\cdot 2.2\cdot 6\cdot c_0^2/(6\pi)} = 0.5\sqrt{(6\cdot c_0)^2} = 0.5\cdot 6c_0 = 3c_0$.

But at the end of this process the real distances are: $6\ c_0 + 2c_0 = 8\ c_0$, and

$c_c = \sqrt{lb/6\pi} = \sqrt{8\cdot 2.2\cdot 6\cdot c_0^2/(6\pi)} = 2.4c_0$, so that the produced crack of $3\,c_0$ is overcritical and the critical process for further fractureis due to an other process. The only possibility is that small crack formation and pro pagation in the remaining intact part of the ligament becomes determining. This determining clear wood failure, which starts at half way the yield drop, is discussed in § 4.7.

For every successive process applies, that every crack merges with one neighbor by extension at one side over a distance of $1\ c_0$, leading to halving of the solid area of the ligament, and to an increase of the crack length by: $2c_{n+1} = 2\cdot 2c_n + 2c_0$, giving $2c_1 = 6c_0$ and $2c_2 = 2\cdot 2c_1 + 2c_0 = 14c_0$, as found before. The increase of the crack length is: $\Delta(2c) = 2c_{n+1} - 2c_n = 2c_n + 2c_0$. Including the initial crack length of $2\,c_0$, the increase of the total crack length is: $\Delta(2c) = 2c_{n+1} - 2c_n - 2c_0 = 2c_n$. (4.21)

More general for all merging cracks at any distance during time Δt this is:

$$\Delta(c) = \beta_1 \cdot c \cdot \Delta t \tag{4.22}$$

and as the determining damage deformation kinetics equation this is (see § 5, eq.5.3):

$$dc/dt = \beta_2 \cdot c_0 \cdot \exp(\sigma\varphi) \tag{4.23}$$

when the initial site concentration c_0 is high, (zero-order reaction) as applies for row A of Fig. 3.

Eq.(4.23) can be written: $\ln(\dot{c}) = \ln(C) + \phi\sigma_v$, or, because $\varphi\sigma_{v0} = n$, is constant, independent of stress, due to

the time stress equivalence, [1], is:

$$\frac{\sigma_v}{\sigma_{v0}} = 1 + \frac{1}{n}\ln\left(\frac{\dot{c}}{\dot{c}_0}\right) \tag{4.24}$$

showing that the combined Griffith – crack-merging model is identical to common damage behavior. Regarding Fig. 4.8, it is clear that the overcritical longer cracks are not determining for crack extension, but that fracture always is due to the same micro crack extension in the remaining intact clear wood parts of $2c$ length. The damage process acts in all these parts at the same time. Thus, for the whole fracture process, from the beginning to full separation, applies, that micro-cracking in the intact part $(b - c)$ of the ligament is determining, and that the concentration is not determined by $c_c = \sqrt{lb / 6\pi}$, but by: $c_c' = \sqrt{c_1(b - 2c)^2 / 6\pi}$ $= c_2(b - 2c)$, (with $c_1 = 2.2^2$, is $c_2 = 0.5$).

The kinetics shows the same behavior as for clear wood, indicating that always the same small-crack propagation is determining. As shown in [1], always two coupled processes act, showing the same time-temperature and the same time-stress equivalence of both. One process, with a very high density of sites, provides the sites of the second low site density process, as follows from a very long delay time of this second macro-crack process at common load levels. (Of course there is no delay time for macro crack extension at a high loading stress level due to the time stress equivalence). The mode I notched specimen, discussed here, also shows the low concentration reaction by the strong yield drop behavior (of the nominal stress). The coupled processes occur for the crack merging processes, where the initial crack length is the reactant and the product is the newly formed crack length what also applies for macro-crack extension due to the crack merging process. The numerous small-cracks, growing towards the macro notch, provide the site for the macro crack to grow as second low concentration reaction process. This failure mechanism applies for every bond breaking process at any level.

4 7 Mode II shear tests

In [6], [7], results of mode II tests, called asymmetric four point bending (AFPB) tests, are given, applied on very long sub-critical initial crack lengths, which clearly represent an identical state of a former yield drop stage, because the measured K_{IIc} -values were a factor 3 to 4 lower than those of the control tests on standard single edge notched beam (SENB) test-specimens. By the standard fracture equation for this case, eq.(4.25), the value of τ_0 and K_{IIc} were obtained in [6], [7], by estimation of the energy release rate G_{II} by the compliance method at different crack lengths and, as control, by the finite element virtual crack closure method. The found too low value of G_c is now not the critical energy release, but simply the minimal elastic energy for crack closure of the very long crack. In the first eq.(4.7) is G_c then the mean crack closure energy per unit crack length, and the derivation in this equation, with $\partial G_c / \partial c = 0$, gives the condition of minimal mean crack closure energy per unit crack length, as minimum potential energy condition as applies for equilibrium, similar to the fracture energy in the ultimate state, giving the meaning of G_c, and of eq.(4.25), for overcritical crack lengths. Thus also in that case applies:

$$K_{IIc} = \tau_0 \sqrt{\pi a_c} \cdot f(a / W) \tag{4.25}$$

This equation can be written, when clear wood shear failure is determining in this shear loaded specimen:

$$\sqrt{\pi a_c} \cdot f(a / W) = \frac{K_{IIc}}{\tau_0} = C_1 \text{ (constant)} \tag{4.26}$$

where τ_0 is the ultimate nominal stress. C_1 is only dependent on dimensions and stiffness factors of the specimen. This is different from the solution in [6], [7]. There the critical value of G_c, in $K_{IIc} = \sqrt{E G_c}$, is chosen to be at the 5 % offset from linearity. The common calculation in [6], [7], based on the assumption that the overcritical initial crack length is still the critical macro crack length, leads to strongly (factor 3 to 4) too low, not critical, not constant, values of G_c. C_1 then is dependent on a / W, and is determined by the compliance method and crack closure technique. This delivered right values of $f(a / W)$.

According to fig.12 of [7], there is no difference (by volume effect) between the data for W = 40 mm and W = 20 mm, thus mean values of both are here regarded.

Determining for small crack extension, at the presence of a long (post-critical) crack, is the still available intact area of: $(W - a)$ $c_1(W - a)$. The critical small crack density is proportional to this area according to eq.(4.13).

Thus, the critical macro-crack length, which is equivalent to the critical small crack density, is:

$$a_c = \sqrt{bl/6\pi} = \sqrt{(c_1 W(1-a/W)\cdot W(1-a/W)/6\pi)} = c_2(1-a/W)\ W \tag{4.27}$$

where: $l = W(1-a/W)$ and $b = c_1 W(1-a/W)$ as St. Venant distance. Thus, because W is constant, is:

For $a/W = 0.7$, is: $\sqrt{a_c}\cdot f(a/W) = c_6\sqrt{(1-a/W)}\ \ f(a/W) = c_6\cdot\sqrt{0.3}\cdot 1.0 = 0.55c_6$ (4.28)

For $a/W = 0.8$, is: $\sqrt{a_c}\cdot f(a/W) = c_6\sqrt{(1-a/W)}\ \ f(a/W) = c_6\cdot\sqrt{0.2}\cdot 1.2 = 0.54c_6$ (4.29)

For $a/W = 0.9$, is: $\sqrt{a_c}\cdot f(a/W) = c_6\sqrt{(1-a/W)}\ \ f(a/W) = c_6\cdot\sqrt{0.1}\cdot 1.67 = 0.53c_6$, (4.30)

giving the necessary constant value of C_1 of eq.(4.26) and providing the control of the empirical $f(a/W)$-values of [6], which are based on the initial macro-crack lengths of a/W = 0.7, 0.8 and 0.9. Eq.(4.28) to (4.30) show, that for this type of test specimen, with overcritical crack lengths, applies:

$$f(a/W) = 0.54/\sqrt{1-a/W} \tag{4.31}$$

Regarding fracture, it is to be expected, that the determining clear wood shear strength is the same for the above 3 cases. Thus: Eq.(4.25) also can be written, expressed in the ultimate actual shear stress:

$$\tau_u = \frac{K_{II}}{\sqrt{\pi a}\cdot f(a/W)}\cdot\frac{W}{W-a} = \frac{K_{II}}{\sqrt{\pi a}\cdot(1-a/W)\cdot f(a/W)} = \frac{K_{II}/\sqrt{\pi W}}{\sqrt{a/W}\cdot(1-a/W)\cdot f(a/W)} \quad \text{or:}$$

$$\tau_u\sqrt{\pi W} = \frac{K_{II}}{\sqrt{a/W}\cdot(1-a/W)\cdot f(a/W)}, \tag{4.32}$$

This is constant (because W also is constant for the 3 cases). Then:

For $a/W = 0.7$, is: $\dfrac{K_{II}}{\sqrt{a/W}\cdot(1-a/W)\cdot f(a/W)} = \dfrac{0.79}{\sqrt{0.7}\cdot 0.3\cdot 1} = 3.2$ (4.33)

For $a/W = 0.8$, is: $\dfrac{K_{II}}{\sqrt{a/W}\cdot(1-a/W)\cdot f(a/W)} = \dfrac{0.71}{\sqrt{0.8}\cdot 0.2\cdot 1.2} = 3.3$ (4.34)

For $a/W = 0.9$, is: $\dfrac{K_{II}}{\sqrt{a/W}\cdot(1-a/W)\cdot f(a/W)} = \dfrac{0.52}{\sqrt{0.9}\cdot 0.1\cdot 1.67} = 3.3$, (4.35)

giving a mean value of: $\tau_u\sqrt{\pi W} = 3.25\ \ \text{MPa}\sqrt{\text{m}}$, and with W = 40 mm, this is τ_u = 9 Mpa of the tested small clear specimen of 40x10x15 mm^3 glued in the centre of beam specimen [7]. Thus $a/W = 0.8$ means that the initial crack length $a = 0.8\cdot 40 = 32$ mm.

The optimal, (quasi critical) $K_{II,m}$ values of 0.79, 0.71 and 0.52 are determined in [6], [7] by the compliance method and the finite element crack closure technique as control, although these values are about a factor 2.5 to 4 below the real critical value. The in [6], [7] found $f(a/W)$-values of 1.0, 1.2 and 1.67, are agreed by eq. (4.28) to (4.30). Because, according to these equations:

$\sqrt{(1-a/W)}\ \ f(a/W) = c_7 =$ constant, is:

$$\frac{K_{II}}{\sqrt{a/W}\cdot(1-a/W)\cdot f(a/W)} = \frac{K_{II}}{\sqrt{a/W}\cdot\sqrt{(1-a/W)}\cdot c_7} = c_8 \quad \text{or:} \quad \frac{K_{II}}{\sqrt{a/W}\cdot\sqrt{(1-a/W)}} = c_9\ .\ \text{Thus:}$$

For $a/W = 0.7$, is: $\dfrac{K_{II}}{\sqrt{a/W}\cdot\sqrt{(1-a/W)}} = \dfrac{0.79}{\sqrt{0.7}\cdot\sqrt{0.3}} = 1.72$ (4.36)

For $a/W = 0.8$, is: $\dfrac{K_{II}}{\sqrt{a/W}\cdot\sqrt{(1-a/W)}} = \dfrac{0.71}{\sqrt{0.8}\cdot\sqrt{0.2}} = 1.77$ (4.37)

For $a/W = 0.9$, is: $\dfrac{K_{II}}{\sqrt{a/W}\cdot\sqrt{(1-a/W)}} = \dfrac{0.52}{\sqrt{0.9}\cdot\sqrt{0.1}} = 1.73$ (4.38)

and for these specimens thus is:

$$K_{II,m} = 1.74\cdot\sqrt{a/W}\cdot\sqrt{1-a/W}\quad \text{MPa}\sqrt{\text{m}} \tag{4.39}$$

which is not based on a critical fracture energy, but on an ultimate, actual, clear wood, shear strength. It thus is confirmed by the data of [6], [7], that the actual mean shear strength of the intact part of the fracture plane is determining and not the, on the macro crack length based, apparent critical K_{II} - value, which is not

constant and too low for macro-crack extension. Macro crack extension is thus due to small crack merging and extension towards the macro-crack tip. There is no principal difference between mode I and mode II fracture, because failure for any stress combination, is due to reaching the ultimate, uniaxial, tensile strength at the crack-boundary near the crack tip [2]. Virtual, oblique, crack extension in the isotropic wood matrix applies for shear and all combined mode I – II failure cases as lower bound solution, which is an exact solution, being equal to the empirical Wu-fracture criterion [2], and thus is the real solution.

4.8. Mode I fracture at overcritical crack lengths

The same equations, as given in § 4 7 for mode II shear tests, apply for mode I tensile behavior for the successive increasing crack lengths by crack merging during yield drop. Thus similar to eq.(4.28) to (4.30) is**:**

For $2a/W = 3/4 = 0.75$, is: $\sqrt{a_c} \cdot f(a/W) = c_6\sqrt{(1-2a/W)}\ f(a/W) = c_6 \cdot 0.5 \cdot 1.51 = 0.75 \cdot c_6$ (4.40)

For $2a/W = 7/8 = 0.875$, is: $\sqrt{a_c} \cdot f(a/W) = c_6\sqrt{(1-2a/W)}\ f(a/W) = c_6 \cdot 0.354 \cdot 2.07 = 0.73 \cdot c_6$ (4.41)

For $2a/W = 15/16 = 0.938$, is: $\sqrt{a_c} \cdot f(a/W) = c_6\sqrt{(1-2a/W)}\ f(a/W) = c_6 \cdot 0.25 \cdot 2.87 = 0.72 \cdot c_6$ (4.42)

where, (see[8]): $f(a/W) = 1/\sqrt{1-(2a/W)^2}$ (4.43)

In [8], the exact derivation, as boundary value problem, of $f(a/W)$ according to eq.(4.43) is given, which does apply for critical crack lengths, while eq.(4.40) to (4.42) show that the relation: $f(a/W) = 0.74/\sqrt{(1-2a/W)}$ applies for overcritical crack lengths. This also applies for overcritical crack lengths of mode II, according to eq.(4.31).

It now can be concluded that the common calculation, where the overcritical crack length is treated as the critical crack length leads to too low, not constant, apparent energy release rates, which represent the minimum energy of crack closure. The same equation with the same values of the apparent release rates and the same values of $f(a/W)$ is found by fracture and clear wood failure of the intact part of the ligament, showing this process to be determining for fracture at lower stresses. Not the critical energy release rate is determining but the maximal stress, that has to follow the Wu-equation in stresses, of in stress intensity factors for zero open crack lengths according to § 6.

V. Deformation kinetics of fracture

The basic equations for fracture according to the limit analysis equilibrium theory of molecular deformation kinetics are given in § 4.4 of [1]. The basic concept of this, fundamental theory is to regard plastic flow as a matter of molecular bond breaking and bond reformation in a shifted position, what is the same as to state that flow is the result of a chemical reaction like isomerization. Thus not the composition changes, but only the bond structure of the molecules. Damage occurs when not all broken side bonds reform, providing the sites for a damage process.

The general theory, developed in [1], is based on the limit analysis equilibrium method and is, as such, an exact approach, which is able to predict all aspects of time dependent behavior of materials by the same constitutive equation, because the mathematical derivation of this general theory is solely based on the reaction equations of the bond-breaking and bond- reformation processes at the deformation sites due to the local stresses in the elastic material around these sites. The form of the parameters in the rate equations, are according to the general equilibrium requirements of thermodynamics. By expressing the concentration and work terms of the rate equation in the number and dimensions of the flow units, the expressions for the strain rate, fracture, flow, hardening and delay time are directly derived without any assumptions. To obtain simplifications, series expansion of the potential energy curve is applied, leading to the generalized flow theory, thus to a proof of this general flow model, and showing the hypotheses of this generalized theory, to be consequences of the series expansion. This theory thus applies generally, also for structural changes, giving an explanation of the existing phenomenological models and laws of fracture.

The rate equation for fracture then can be given, for high stress, as applies for fracture, by:

$$-\frac{d\rho}{dt} = \frac{2\rho}{t_r}\sinh\left(\frac{W}{kT}\right) \approx \frac{\rho}{t_r}\exp\left(\frac{W}{kT}\right) \tag{5.1}$$

where the concentration of activated units per unit volume ρ can be written: $\rho = N\lambda A/\lambda_1$ .with: N flow units per unit area of a cross section, each at a distance λ_1 behind each other, with λ as jump distance and A as area of the flow unit. The work of a flow unit W, with area A moving over a barrier, over a distance λ is: $W = fA\lambda = \sigma\lambda/N$. Because of equilibrium, per unit area, of the external load $\sigma \cdot 1 \cdot 1$ with the force on the N

flow units: NfA. Thus $\sigma = NfA$ and eq.(5.1) becomes, expressed in the nominal, macro, engineering stress σ, which is the part of the total external stress, that acts on *N*, to be found from tests with different loading paths:

$$-\frac{d}{dt}\left(\frac{N\lambda}{\lambda_1}\right)=\frac{N\lambda}{\lambda_1 t_r}\exp\left(\frac{\sigma\lambda}{NkT}\right), \tag{5.2}$$

In this equation is t_r the relaxation time. The value of *A* can be regarded constant because any change is compensated by an corrected value of f and a corrected value of λ to obtain a correct load on the flow unit and its correct volume. Eq.(5.2) can be written, with $N' = N/\lambda_1$ (the number of flow units per unit volume): $-d\left(N'\lambda\right)/dt = \left(N'\lambda/t_r\right)\exp\left(\sigma\lambda/NkT\right)$, or:

$$\frac{d}{dt}\left(\frac{\lambda}{N'}\right)=\frac{\lambda}{N' t_r}\exp\left(\frac{\sigma\lambda}{NkT}\right) \tag{5.3}$$

For this zero order reaction in wood, when the very high initial reactant concentration does not change much, the solution is:

$$\frac{\lambda}{N'}=\frac{\lambda t_f}{N_0' t_r}\exp\left(\frac{\sigma\lambda}{N_0 kT}\right)+\frac{\lambda}{N_0'}, \text{ or:}$$

$$\left(\frac{\lambda}{N'}-\frac{\lambda}{N_0'}\right)\cdot\frac{N_0'}{\lambda}=\frac{t_f}{t_r}=\frac{t_f}{t_0}\cdot\frac{kT}{\upsilon h}\exp\left(-\frac{E}{kT}+\frac{\sigma\lambda}{N_0 kT}\right)=\frac{t_f}{t_0}\cdot\exp\left(-\frac{E}{kT}+\frac{\sigma\lambda}{N_0 kT}\right) \quad \text{or} \quad (\text{with } \frac{kT}{h\nu}=1):$$

$$\frac{E}{kT}-\frac{\sigma\lambda}{N_0 kT}=\ln\left(\frac{t_f}{t_0}\right)-\ln\left(\frac{N_0'}{N_f'}-1\right)=\ln\left(\frac{t_f}{t_0}\right), \tag{5.4}$$

This last, according to Fig. 5, which applies for structural materials. Thus $N_f' = 0.5\cdot N_0'$ as also experimentally found for fracture, i.e. the crack length is about the crack distance, or the intact area has reduced to 0.5 times the initial area when macro-crack propagation starts due to small crack merging behavior, which explains the measured mode I and mode II final nominal yield drop behavior of fracture.

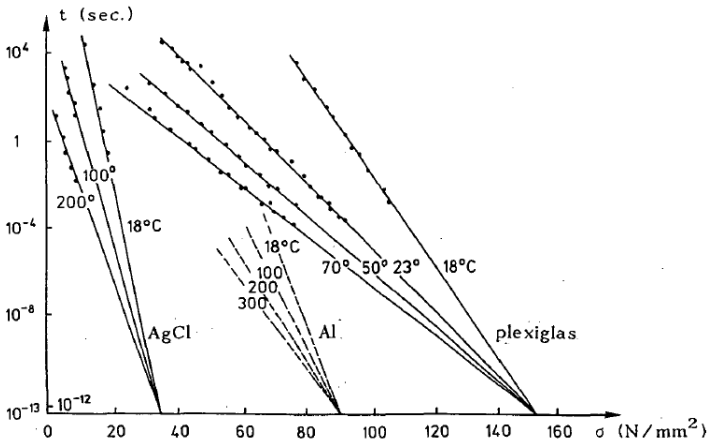

Figure 5. Stress and temperature dependence of the lifetime for structural materials [1]

VI. Small crack limit strength behavior

The interpretation of Fig. 6 in literature is to regard the inclined line to represent LEFM theory, the horizontal line to be the strength theory and the curved, connecting line to follow nonlinear fracture theory. However, there is no difference between nonlinear and linear elastic (LEFM) fracture mechanics. For both the linear elastic - full plastic approach of limit design applies. The full-plastic zone of the elastic-full plastic approach exists, as failure criterion, by a single curve in stress space as shown in Fig. 6. In this figure of [9], is d/d_0, the ratio of specimen size to the fracture process zone size. But, because the line is the result of volume effect tests, the initial crack length is proportional to the test-specimen length. Thus, d/d_0 also can be regarded to be the ratio initial open crack length to the process zone size (times a factor). Then, for small values of *d*, this d/d_0 ratio

also may represent the critical small crack density in a macro specimen (d also is crack interspace). The curved line of Fig. 6, follows the equation:

$$\ln \sigma = \ln \sigma_0 - 0.5 \ln (1 + d / d_0) \tag{6.1}$$

This can be written:

$$\ln \left| \frac{\sigma}{\sigma_0} \right| = \ln \left| \frac{d_0 + d}{d_0} \right|^{-0.5} = \ln \left| \frac{d_0}{d_0 + d} \right|^{0.5} \tag{6.2}$$

or: $\sigma \sqrt{d_0 + d} = \sigma_0 \sqrt{d_0} = K_c / \sqrt{\pi}$, (6.3)

This confirms that the curve represents the stress intensity as ultimate state with K_c as critical stress intensity factor as should be for values of d / d_0 >>1. For these higher values the curved line approaches the drawn straight tangent line $\ln \sigma = \ln \sigma_0 - 0.5 \cdot \ln (1 + d / d_0) \approx \ln \sigma_0 - 0.5 \ln (d / d_0)$ with the necessary slope of the curve $\frac{\partial \ln(\sigma / \sigma_0)}{\partial \ln(d / d_0)} \approx -0.5$ as limit. The real slope however is:

$$\frac{\partial \ln \sigma}{\partial \ln(d / d_0)} = \frac{\partial \ln(\sigma / \sigma_0)}{(d_0 / d)\partial(d / d_0)} = \frac{d}{d_0} \frac{\partial \left(\ln (1 + d / d_0)^{-0.5} \right)}{\partial (d / d_0)} = \frac{d}{d_0} \cdot \frac{-0.5}{1 + d / d_0} = \frac{-0.5}{1 + d_0 / d} \tag{6.4}$$

This slope is: – 0.5 for $d >> d_0$ and this slope is zero when $d = 0$. This shows that for the whole curve LEFM applies and it is an indication that, at zero crack dimensions, thus for: d = 0, the clear wood strength theory still follows LEFM, because it applies also for the constant initial length d_0. After first yield drop, to half way unloading, the strength theory applies for further crack extension. Similar to steel, where yield drop follows after dislocation multiplication and breakaway, applies for wood the fracture zone d_0 formation, and small crack propagation. The Wu-equation then applies in stresses [2] in stead of in stress intensities.

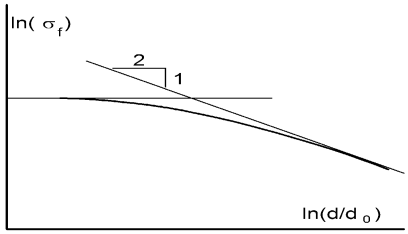

Fig. 6. From [9]. Limit LEFM behavior as correction of the interpretation of [9].

VII. Application of the singularity J-integral approach

Outer the standard methods for estimation of the energy release rate, the application of the *J*-integral (Rice integral) and *M-θ*-integral are becoming more and more a must for the singularity approaches for wood. However, the finite element applications appear to lead to quite different outcomes by different authors, showing the application to be not exact, as also follows from the following remarks, found in literature. *J* (around a singularity) is the component along the crack-line of a vector integral, having a meaning for not oblique, (thus *impossible* for shear and mixed mode [2]) and (*only for mode I*) incipient self-similar growth of a crack in a (nonlinear) elastic material. In this case, *J* has the meaning of the rate of energy-release per unit of crack-extension. The path-independency of *J* can be established only, when the strain energy density (or stress working density) of the material is a single valued function of strain. In a deformation theory of plasticity, which is valid for radial monotonic loading but *precludes unloading* and which is mathematically equivalent to a nonlinear theory of elasticity, *J* still characterizes the crack-tip field and is still a path-independent integral. However, in this case, *J* does not have the meaning of an energy-release rate; it is simply the total potential-energy difference between two identical and identically (monotonically) loaded cracked bodies which differ in crack lengths by a differential amount. Further, in a flow theory of plasticity (*as applies for wood*}, even under monotonic loading, the path-independence of *J* cannot be established. Also, under arbitrary load histories which may include loading and unloading, *J* is not only not path-independent, but also does not have any physical meaning. The blunting of the top of the loading curve and formation of the fracture zone and the main amount of crack growth with crazing and small crack formation in, (and outside), the process zone, means unloading and non-proportional plastic deformation which also invalidates the deformation theory of plasticity.
Thus the *J*- integral method, of the singularity approach, does not apply to wood.

VIII. Conclusions

- "Strain softening" called, yield drop is elastic unloading of the actual elastic stress at the intact part of the specimen, outside the fracture zone (and thus is not softening, as strain induced material transformation).
- The assumption of strain softening of the fracture stress is based on the error to regard the nominal stress to be the actual, ultimate stress, at the actual area of the fracture plane. This illogic assumption is automatically rejected because it is against fundamental properties and constitutive laws of mechanics.
- Thus, "softening"- called yield drop only exists for the nominal stress and not for the actual fracture stress, which shows hardening. The Griffith stress: $\sigma_c = \sqrt{G_c E / \pi c}$ is a nominal stress, acting on the section $b \cdot t$ of Fig. 4.1. The Griffith stress therefore only has the meaning to be the actual stress, of the intact, not fractured, not ultimate, but elastic loaded, part of this specimen, which shows yield drop at crack extension, as is common, for processes with a low reactant concentration, thus, in this case, containing a single extending macro-crack.
- This yield drop unloading, necessary for equilibrium, is due to decrease of the stiffness and increase of damage at the fracture site. The real, statically admissible, actual mean stress at the fractured region shows necessarily real and apparent hardening (by the spreading effect).
- Yield drop only is possible at a constant strain rate test, thus is not possible in a constant loading rate test and also not in a dead load to failure test. Softening called yield drop, which is elastic unloading of the intact, not ultimately loaded, part of the specimen, thus is not a material property.
- It is discussed that the fictitious crack models and the cohesive zone models are too far from theory to have any meaning. By not regarding the actual real stress, at the fracture plane, also the equilibrium, compatibility, normality, yield and boundary conditions at the crack boundary are not satisfied.
- As known from Continuum damage mechanics and Deformation kinetics, it is necessary to apply the actual stress on the actual area in damage and fracture equations, for right results, as follows from the uncountable number of solutions, which are confirmed by tests. Limit analysis, based deformation kinetics [1], has to be applied, (e.g. in continuum mechanics), for exact solutions, giving the possibility to design, reliable new, never tested, structures and to account for the influence of time (duration of load), moisture content and temperature.
- Fracture of the ligament does only at the start of yield drop follows the Griffith theory and thus is total fracture not due to single macro crack propagation alone. After half way the yield drop unloading of the nominal stress, the apparent energy release rate is not high enough anymore. Further crack extension follows a small rack merging mechanism and macro crack extension is due to small-crack propagation toward the macro-crack tip. This is caused by clear wood failure following an ultimate stress failure criterion.
- According to the crack merging mechanism and according to molecular deformation kinetics there is a critical small crack density, when the crack distance is about the crack length, for the start of yield drop.
- Important is the conclusion that, after the start of yield drop, according to a critical energy release rate, further crack extension follows by an ultimate mean shear strength criterion of the intact part of the fracture plane.
- Small-crack merging explains precisely the "softening" called yield drop curve (of [5]).

References

[1] T.A.C.M. van der Put. Deformation and damage processes in wood, , Delft University Press The Netherlands, (1989). B(1989a).

[2] T.A.C.M. van der Put. A new fracture mechanics theory of wood, Nova Science Publishers NY, or more complete:: T.A.C.M. van der Put Exact and complete Fracture Mechanics of wood Theory extension and synthesis of all series C publications

[3] L.M. Kachanov. Introduction to Continuum Damage Mechanics, , Martinus Nijhoff Publishers, Dordrecht

[4] T.A.C.M. van der Put. Derivation of the bearing strength perpendicular to the grain of locally loaded timber blocks Holz Roh Werkst (2008) 66: 409–417

[5] L. Boström, Method for determination of the softening behaviour of wood etc. Thesis, Report TVBM-1012, Lund, Sweden, (1992).

[6] Yoshihara, H. (2012) Mode II critical stress intensity factor of wood measured by the asymmetric four-point bending test of single- edge-notched specimen while considering an additional crack length, Holzforschung, 66, pp 989-992.

[7] Yoshihara H. (2008) Mode II fracture mechanics properties of wood measured by the asymmetric four-point bending test using a single-edge-notched specimen, Eng. Frac. Mech. 75 pp.4727-4739.

[8] T.A.C.M. van der Put. Exact Derivation of the Geometric Correction Factor of the Center Notched Test Specimen, Based On Small Cracks Merging As Explanation of Softening , Int J Comput Eng Res (IJCER) Vol. 04, Issue 7, July 2014.

[9] I. Smith, E. Landis, M. Gong, Fracture and Fatigue in Wood, J. Wiley & Sns.